European Polymer Journal 143 (2021) 110210

Contents lists available at ScienceDirect

European Polymer Journal

journal homepage: www.elsevier.com/locate/europolj

Formaldehyde-doxorubicin dual polymeric drug delivery system for higher efficacy and limited cardiotoxicity of anthracyclines

Estela Ordonez [a], Laken L. Kendrick-Williams [a,b], Eva Harth [a,*]

[a] Department of Chemistry, Center of Excellence in Polymer Chemistry (CEPC), University of Houston, 3585 Cullen Blvd, Houston, TX 77030, USA
[b] Department of Chemistry, Vanderbilt University, 7665 Stevenson Center, Nashville, TN 37235, USA

ARTICLE INFO

2010 MSC:
00–01
99–00

Keywords:
DOX
Formaldehyde
Nanosponge
Cardiotoxicity

ABSTRACT

We report the synthesis of a dual delivery system composed of chemically bound pH-responsive formaldehyde polymer prodrugs and pH-responsive doxorubicin loaded nanoparticles to increase the therapeutic index of doxorubicin by working in synergy with formaldehyde to enable the formation of DOX-DNA adducts and limiting the cardiotoxicity of anthracyclines. Polyacrylates bearing 1,2- and 1,3- pendant diols were synthesized via reversible addition fragmentation chain transfer (RAFT) polymerization to conjugate formaldehyde, forming 5- or 6-membered acetal rings with tunable conjugation percentages (1.5–10 wt%) for controlled release in acidic environments of the tumor extracellular matrix. The formaldehyde-conjugated prodrugs are then combined with polyester nanoparticles formed by intermolecular crosslinking via oxime click chemistry of less than 200 nm in size containing 14 wt% encapsulated Doxorubicin (DOX). Release kinetics show a sustained release of both DOX and formaldehyde at pH 5.0, mimicking the low pH of the tumor environment whereas insignificant release was recorded at physiological pH. The cell viability of the dual delivery system combination was evaluated in 4 T1 breast cancer cells resulting in a considerably increase of cell death of about 4-fold compared to free DOX alone. The protective effect of formaldehyde towards DOX- induced damages was observed in Lactate dehydrogenase assays with cardiomyocytes (P1-3). The resulting polymeric delivery system is the first reported example of a DOX and formaldehyde co-administration, demonstrating the potential significant effect of formaldehyde towards an improved anti-cancer efficacy and reduced cardiotoxicity of DOX.

1. Introduction

The implementation of synergistic drug therapies into the clinic is widely accepted due to enhanced efficacy [1], reduced dosage requirements, and decreased toxicity [2] of the individual drug components. Specifically Doxorubicin (DOX), a broad spectrum anti-tumor antibiotic is known to develop chemo resistance [3] like many other anthracycline-based therapeutics and moreover its clinical use is limited by acute and chronic cardiotoxicity [4–6]. The DOX-induced cardiotoxicity is attributed to the generation of reactive oxygen species (ROS) and the formation of the toxic metabolite doxorubicinol [7,8] as result of some of the main molecular events that damage cardiomyocytes, cardiac muscle cells, and can lead to heart failure many years after treatment [9]. Therefore, it is prevalent to seek non-overlapping mechanisms of action in drug combinations with doxorubicin to avoid resistance, increasing the sensitivity of the therapeutic and improving the therapeutic index by protection of the cardiac system.

It has been reported that a family of acyloxyalkyl prodrugs release butyric acid and formaldehyde upon metabolic hydrolysis and can act in synergy with doxorubicin to increase substantially the formation of DOX-DNA adducts, DOX's primarily intercalation complex as its active anti-cancer mechanism [6,10–14]. DOX-DNA adducts do not only enhance the therapeutics efficacy by 3–4 fold [15] but also reduce cardiotoxicity [10]. It is postulated that formaldehyde reacts with doxorubicin to form a DOX—N = CH_2 Schiff's base which is readily reacting with the amino groups on the guanine in GpC DNA sequences [16,17]. Doxorubicin is thereby sequestered, preventing DOX cycling and enzymatic degradation to generate ROS and the toxic metabolite, while attenuating at the same time cancer cell growth by forming the desired DOX-DNA adduct [10]. It is to note that metabolized free formaldehyde has not shown any adverse toxicity [10]. This finding and others has inspired the synthesis of doxorubicin-formaldehyde conjugates and several prodrugs such as Doxoform (DoxF), and Doxsaliform (DoxSF) have been produced and tested [15–18]. In addition to the

* Corresponding author.
E-mail address: harth@uh.edu (E. Harth).

https://doi.org/10.1016/j.eurpolymj.2020.110210
Received 11 October 2020; Received in revised form 11 December 2020; Accepted 14 December 2020
Available online 19 December 2020
0014-3057/© 2020 Elsevier Ltd. All rights reserved.

aforementioned benefits of this drug combination, a higher uptake into multi-drug resistant MCF-7/Adr cells was also reported [16]. While these are promising results, the acyloxyalkyl ester prodrugs and Dox-formaldehyde prodrugs release formaldehyde by hydrolysis and metabolize very quickly with the stability and shelf-life of an aqueous therapeutic solution being limited to a few minutes [15].

We sought to design a dual pH-responsive delivery system for formaldehyde and doxorubicin that exemplifies a release mechanism for formaldehyde and DOX using pH-responsive materials to trigger the release in the tumor extracellular matrix that is known for having a higher acidity than other tissues [19–21]. Polymer prodrugs seemed ideal as they can bind a multitude of small molecules and the binding of gaseous compounds is known for other attempts to enable a controlled release from a stable carrier. For example, carbon monoxide [22,23] and nitric oxide [24–26] have been studied to increase the potency of other chemotherapeutics or to reverse multidrug resistance.

Thus, to design a formaldehyde-DOX dual drug delivery system, we opted to use a polymeric prodrug-nanoparticle combination, in which the formaldehyde is bound to an acrylate based hydrophilic polymer and the formaldehyde can be conjugated in varied percentages. As ideal monomers, we chose solketal acrylate (1,2-diol) and 2-(acryloyloxy) ethyl2,2,5-trimethyl-1,3-dioxane-5-carboxylate diol (1,3-diol) which upon reaction with formaldehyde forms the corresponding acetal derivative resulting in 5– and 6–membered rings. Here, we aimed to explore if the ring size has an effect on the kinetics of the ring cleavage to release formaldehyde. For Doxorubicin, we selected a sustained nanoparticle delivery system that could be combined with the polymeric prodrug. In our previous work, we reported on a nanoparticle which is crosslinked by forming ketoxime linkages, derived from a reaction of 2-oxepane-1,5-dione (OPD)-containing polyesters in the backbone of the polymer [27]. Upon full reduction of the ketoximes, the nanoparticles will contain alkoxyamine units and differences in release kinetics of hydrophobic drugs were observed. For this work, we aimed to investigate partially reduced particles, containing 50% ketoxime and 50% alkoxyamine crosslinks. We hypothesized that doxorubicin, being a hydrophobic drug, would benefit from a release system designed for a faster release, close to the expected rapid release of formaldehyde from the prodrug.

In this report, we present the synthesis of the first pH- responsive dual delivery system with a concerted delivery of both formaldehyde and doxorubicin. Two formaldehyde-polymer prodrugs forming acetal functionalities were prepared by reversible addition fragmentation chain transfer (RAFT) polymerization with the gaseous compound to test for tailoring release profiles. Secondly, a crosslinked polyester nanoparticle was designed and synthesized for the delivery of doxorubicin with fast release kinetics (Fig. 1). Release kinetics by a Purpald® colorimetric assay identified the five-membered acetal ring be slightly favorable for release at pH 5.0 over physiological pH and cell toxicity

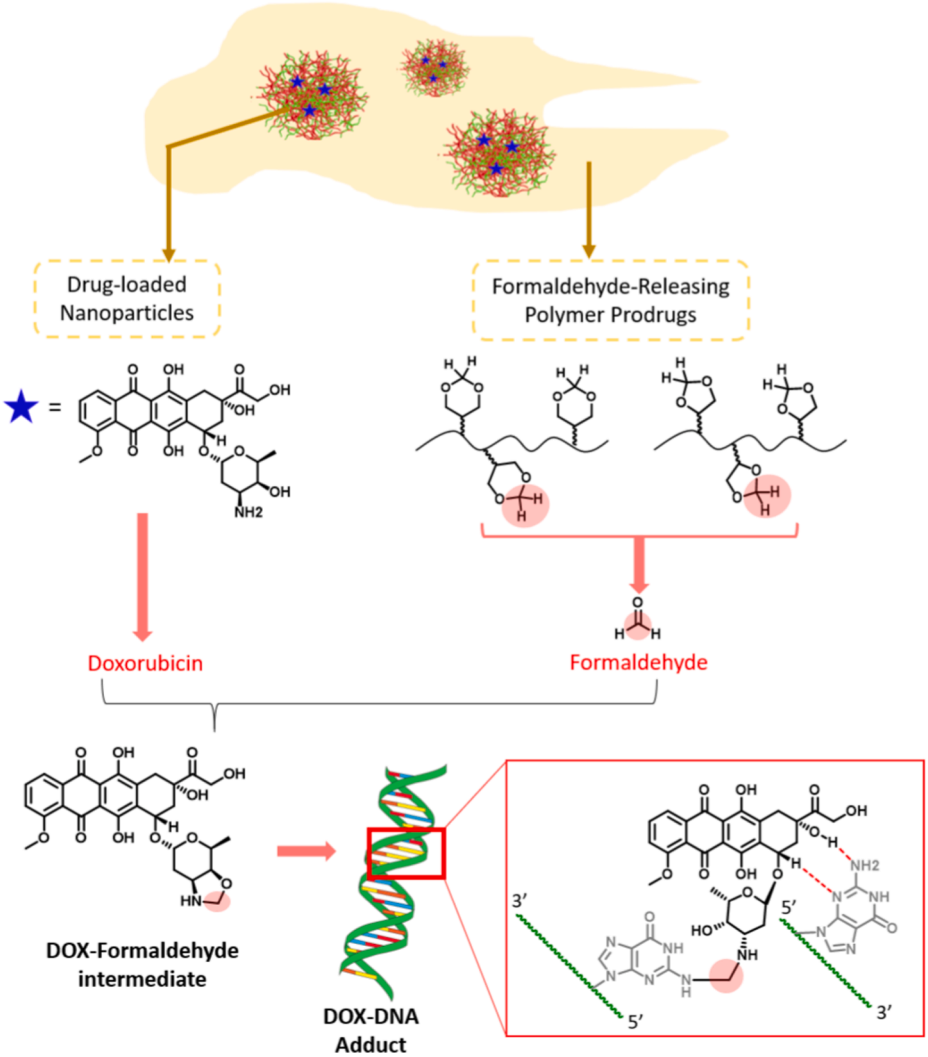

Fig. 1. Resulting polymeric matrix composed of formaldehyde-releasing polyacrylate prodrugs and DOX-loaded partially reduced ketoxime/alkoxyamine polyester nanoparticles forming the DOX-Formaldehyde intermediate and DOX-DNA adducts.

studies with mammalian breast cancer 4 T1 cells and neonatal rat ventricular myocytes were conducted. The effect of sustained and synergistic delivery is indicative of the formation of DOX-DNA adducts and results into a higher therapeutic index and limited cardiotoxicity of DOX.

2. Materials and methods

2.1. Materials

All reagents were purchased from Millipore Sigma, Tokyo Chemical Industry America, or Fisher Scientific and used without further purification unless otherwise specified. The 4T1 cell line was purchased from ATCC and the NRVM (P1-3) cell line was purchased from Lonza Bioscience Solutions. Methoxy PEG acrylate was passed through a column of inhibitor remover prior to polymerization. Spectra/Por® dialysis tubing (MWCO = 1000 Da) and Float-a-Lyzer® (MWCO = 0.1–0.5 kDa) were purchased from Spectrum Laboratories Inc. 2-(n-butyltrithiocarbonate)-propionic acid was prepared according to literature [28]. ^{1}H and ^{13}C NMR spectra were recorded on JEOL ECX-400 and JEOL ECA-600 II spectrometers. Chemical shifts were referenced to solvent resonance signals. Gel permeation chromatography (GPC) was conducted on a ToSOH EcoSEC HLC-8320GPC system equipped with a refractive index detector, UV-8320 detector, and TSKgel HHR columns (7.8 × 8300mm G5000HHR, G4000HHR, and G3000HHR) with *N*-dimethylformamide (DMF) as the eluent at a flow rate of 1 mL/min. High performance liquid chromatography (HPLC) analysis of drug concentration was conducted using a Thermo Fisher Ultimate 3000 HPLC system and Phenomenex column (Luna 5μ C8(2) 100 Å, 150 × 4.6 mm, 5 μm) with a gradient solvent system of 100% A to 30% A:70% B over 12 min. Solvent A was water with 1% trifluoracetic acid (TFA), and solvent B was 90% acetonitrile/10% water with 1% TFA. The column was maintained at 35 °C and the absorbance was measured at 475 nm. Transmission electron microscopy (TEM) was perform using JEOL JEM-210F microscope operated at 200 kV. Samples for the transmission electron microscope (TEM) were prepared by dissolving nanoparticles (~2.0 mg) in 0.22 μm filtered acetonitrile (ACN) and stained with 3 drops of 3% phosphotungstic acid monohydrate. Ultrathin Carbon Type-A 400 Mesh Copper Grids were prepared by dipping into the sample solution three times and allowing to dry at room temperature overnight. Dynamic Light Scattering (DLS) was measured on a Malvern Zetasizer Nano system with a fixed angle of 173° at 25 °C using the Molecular Weight function. The sample solutions were made in a 0.1 mg/mL concentration in 0.22 μm filtered tetrahydrofuran (THF). Colorimetry assays were measured using a microplate absorbance reader Perkin Elmer HTS 7000 Bio Assay Reader at 495 nm.

2.2. Methods

2.2.1. Prodrugs synthesis and characterization

To a sealed 1-dram vial, solketal acrylate (1,2-DA, 100 mg, 0.595 mmol) or 2-(acryloyloxy)ethyl2,2,5-trimethyl-1,3-dioxane-5-carboxylate (1,3-DA, 1.33 g, 2.7 mmol), methoxy PEG acrylate (1.03 g, 2 mmol), and 2-(n-butyltrithiocarbonate)-propionic acid (BTPA, 27.6 mg, 0.116 mmol), with azobisisobutyronitrile (AIBN, 1.9 mg, 12 μmol) were dissolved in degassed DMSO in a 1:1 monomer:DMSO ratio, and the mixture was degassed for 20 min. The reaction was heated at 65 °C for 7 h then transferred to dialysis tubing (MWCO = 1000 Da) and dialyzed against 1:1 mixture DCM:MeOH for 24 h (Fig. 2). (1.12 g, 98%, Mn = 12 kDa, Mw = 13.9 kDa, Đ = 1.15, MPEGA = 80%, 1,2-DA = 20%) ^{1}H NMR (600 MHz, $CDCl_3$) δ (ppm): 0.93 (3H, t, —$S(CH_2)_3CH_3$), 1.39 (6H, d, CH_3), 1.63 (s, CH), 1.90 (s, CH), 2.29 (s, CH), 3.37 (s, —OCH_3), 3.55 (t, —O═$COCH_2$—), 3.64 (s, —OCH_2CH_2O—), 4.15 (s, —O═$COCH_2$—), 4.23 (s, —O═$COCH_2$—), 4.31 (s, —O═$COCH_2$—). (243 mg, 67%, Mn = 11.0 kDa, Mw = 12.8 kDa, Đ = 1.17, MPEGA = 67%, 1,3-DA = 33%) ^{1}H NMR (600 MHz, $CDCl_3$) δ (ppm): 0.93 (3H, t, —$S(CH_2)_3CH_3$), 1.19 (3H, s, CH_3), 1.39 (6H, d, CH_3), 1.63 (s, CH), 1.90 (s, CH), 2.29 (s, CH), 3.37 (s, —OCH_3), 3.55 (t, —O═$COCH_2$—), 3.64 (s, —OCH_2CH_2O—), 4.15 (s, —O═$COCH_2$—), 4.23 (s, —O═$COCH_2$—), 4.31 (s, —O═$COCH_2$—) (Figs. S1, S4-S5).

2.2.2. Polymer deprotection

To a 1-dram vial with a stir bar, P(MPEGA-*co*-1,2-DA) (600 mg, 0.388 mmol acetonide) was dissolved in DI water (1.5 mL). Trifluoroacetic acid (11.88 μL, 0.115 mmol) was added and the reaction stirred for 18 h. The solution was transferred to dialysis tubing (MWCO = 1000 Da) and dialyzed against MeOH for 8 h. The polymer was concentrated and dried in vacuo. (480 mg, 80%). Deprotection was confirmed by ^{1}H NMR. Procedure conditions are the same for P(MPEGA-*co*-1,3-DA) (Fig. 3).

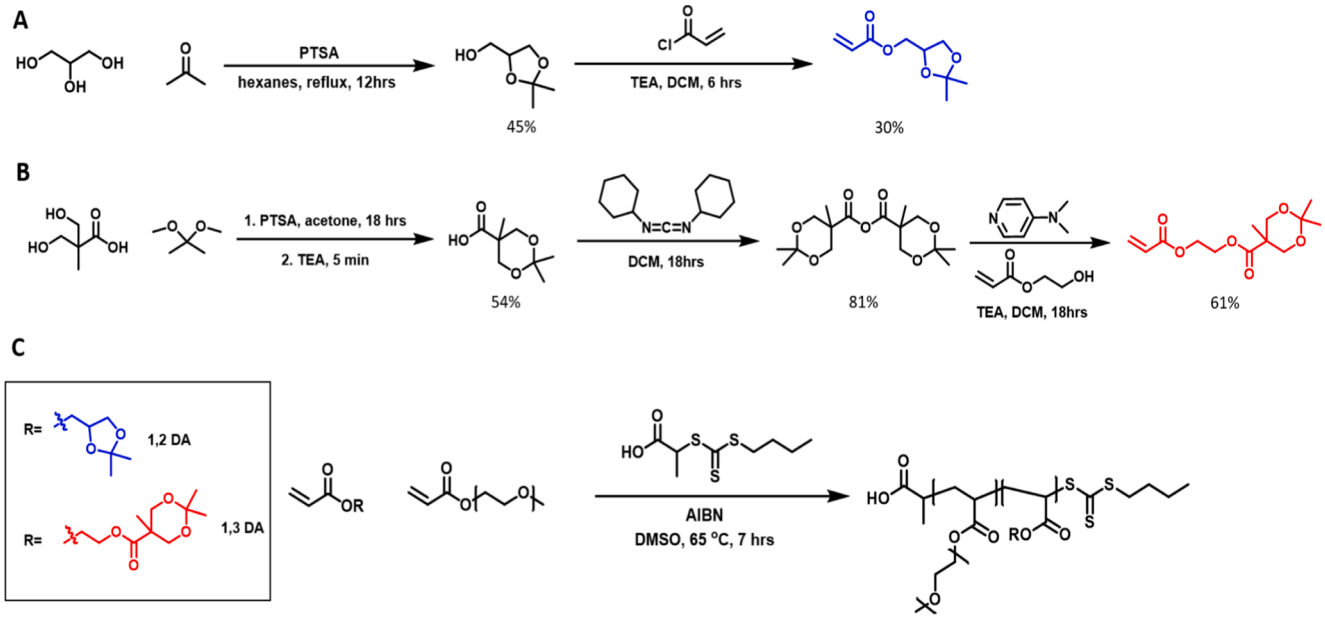

Fig. 2. (A) Synthesis of monomer solketal acrylate (1,2DA), (B) synthesis of monomer 2-(acryloyloxy)ethyl2,2,5-trimethyl-1,3-dioxane-5-carboxylate (1,3DA), and (C) RAFT polymerization to form polyacrylate derivatives with protected diols.

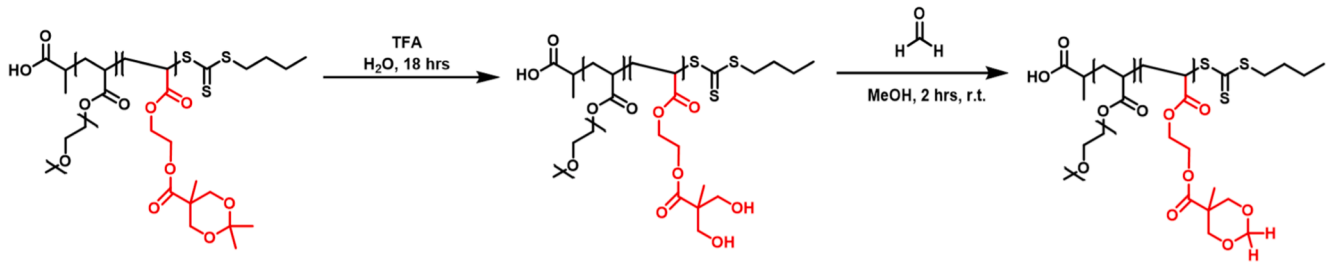

Fig. 3. Deprotection step of polyacrylate P(MPEGA-*co*-1,3DA) and formaldehyde attachment to yield the resulting prodrug CHO-P(MPEGA-*co*-1,3DA). Same conditions were used for P(MPEGA-*co*-1,2DA).

2.2.3. Formaldehyde attachment to form prodrugs

Deprotected P(MPEGA-*co*-1,2-DA) (200 mg, 1 equiv.) was weighed into a 1-dram vial with stir bar. Formaldehyde solution (37 wt% in water, 241 μL, 6 mmol, 50 equiv./diol) was added to the reaction vial, and the mixture was stirred at room temperature for 2 h. Methanol was removed under rotary evaporation and then resuspended in cell culture grade water and filtered using ultra centrifugal filters (MWCO = 3 kDa). Samples were centrifuged at 14 K rpm for 40 min to remove formaldehyde oligomers and the filtrate discarded. The collected material in cell culture grade water was lyophilized. The product was collected and stored at 4 °C until used. Attachment was confirmed by ^{1}H NMR and HSQC (Fig. S6). Procedure conditions are the same for deprotected P (MPEGA-*co*-1,3-DA) (Fig. 3).

2.2.4. In vitro release of formaldehyde from prodrugs

Release of formaldehyde from the prodrugs was determined by a colorimetric assay. The samples were prepared through Float-A-Lyzer® dialysis tubing (MWCO: 0.1 K-0.5 K). A sample of prodrug (10.0 mg) was suspended in 1.0 mL of either acidic buffer (NaOAc-acetic acid, pH 5.0) or PBS (pH 7.4) and transferred to a Float-A-Lyzer® dialysis pod. The pod was then placed in a 50-mL Falcon tube containing 18.0 mL of the corresponding buffer solution. Falcon tubes were placed in an oil bath at 37 °C and media was stirred constantly using a magnetic stir bar. Samples of 100 μL were withdrawn from the sink at 0.5, 1, 1.5, 2, 4, 6, 24, 48, 72 h and every two days following. An equal amount of fresh media was added to the sink after each withdrawal to maintain sink conditions. The amount of formaldehyde released at each time point was quantified using a Purpald® colorimetric assay. A 50 μL aliquot of sample was placed in the well of a 96-well plate and 50 μL of 2 mM NaIO4 in 0.2 M NaOH was added to the sample. The plate was then incubated for 20 min at room temperature in the dark. After 20 min, 100 μL of a 34 mM solution of 4-amino-3-hydrazino-5-mercapto-1,2,4-triazole (Purpald®) in 2 M NaOH was added to the sample and incubated at room temperature for 20 min. Finally, 100 μL of a 33 mM NaIO4 in 0.2 M NaOH was added to each well for color development. The absorbance was measured at 550 nm immediately and formaldehyde concentration in each sample was determined against a standard curve.

2.2.5. Synthesis of partially reduced ketoxime/alkoxyamine nanoparticles

P(VL-*co*-OPD) (8% OPD, 150 mg, 3722.12 g mol-1, 3.67 × 10^{-4} mol) was dissolved in dichloromethane (134.2 mL) then added to a 200 mL round bottom flask. O,O'-(((oxybis(ethane-2,1-diyl))bis(oxy))bis (ethane-2,1-diyl))bis(hydroxylamine) (82.4 mg, 1.71 × 10^{-5} mol, 1 equiv.) was dissolved in dichloromethane (2.0 mL) and added quickly to the polymer solution at a fast vortex. After 2 h, sodium cyanoborohydride (11.56 mg, 3.67x10-4 mol, 0.5 equiv.) and a catalytic amount of saturated sodium bicarbonate solution (300 μL) were added directly to the reaction flask. The reaction stirred for 2 h then was transferred to Thermo Scientific™ SnakeSkin™ 10 K MWCO Dialysis Tubing. The solution was dialyzed against a 1:1 mixture of MeOH/DCM for 48 h, with 3–4 solvent changes per day. The solution was filtered with a 0.45 μm filter to remove solid salt particulates and solvent was removed via rotary evaporation. The product was dried in vacuo to yield a light tan waxy solid (80% yield). ^{1}H NMR (400 MHz, $CDCl_3$): δ (ppm): 0.90 (d, 6H); 1.6–1.75 (m); 2.23–2.43 (m); 2.25–2.7 (m); 2.7–2.84 (m); 3.4 (t); 3.65 (m); 4.0 (t); 4.3–4.4 (m). ^{13}C NMR (600 MHz, $CDCl_3$): δ 21.32, 25.53, 28.00, 33.62, 63.85, 67.88, 173.26 (Figs. S8 and S9).

2.2.6. DOX encapsulation

DOX (15.0 mg) was solubilized in dimethyl sulfoxide (DMSO) (45 μL) in a 1.5 mL centrifuge tube. Nanoparticles (60.0 mg, 8% OPD, 2.7 mM, ~140 nm) were added to the DOX centrifuge tube and an additional 155 μL DMSO were added to solubilize the mixture. The mixture was divided equally into 6 1.5 mL centrifuge tubes, approximately 25 μL each. Cell culture grade water containing 1% D-α-tocopherol polyethylene glycol 1000 succinate (1 mL) was added to each centrifuge tube and vortexed to induce DOX encapsulation. D-α-tocopherol polyethylene glycol 1000 succinate is added to coat the particles during encapsulation and aid in resuspension in aqueous media during drug release studies. The mixture was then centrifuged at 14,000 RPM for 40 min. The supernatant was decanted, fresh cell culture grade water (1 mL) was added to the particle pellet and vortexed until particles were resuspended. Centrifugation was repeated at 14,000 RPM for 40 min, then the supernatant was decanted to remove any nonincorporated drug. Cell culture grade water (0.5 mL) was added to the mixture, frozen, and lyophilized to produce DOX-loaded nanoparticles (DOX-NP). HPLC analysis confirmed encapsulation of DOX at an average of 14 wt% with 68% efficiency.

2.2.7. In vitro release of DOX

DOX-loaded nanoparticles were suspended in 1 mL of either sodium acetate-acetic acid buffer (pH 5) or PBS (pH 7.4) containing 0.1% v/v Tween-80 as a surfactant. The suspended DOX-NP were transferred to Float-a-Lyzer® dialysis pod (MWCO: 1000 kD). The pods were placed into 50-mL Falcon tube containing 18 mL of the corresponding release media. Falcon tubes were placed in an oil bath at 37 °C and media was stirred constantly using a magnetic stir bar. Samples of 150 μL were collected from the sink after 1, 2, 4, 6, 24, 48 and 72 h. An equal amount of fresh media was added to the sink after each sample withdrawal to maintain sink conditions. The amount of DOX released was quantified using HPLC at 475 nm and 35 °C with a gradient solvent system of 100% A to 30% A:70% B over 12 min. Solvent A was water with 1% trifluoracetic acid (TFA), and solvent B was 90% acetonitrile/10% water with 1% TFA.)

2.2.8. Cell viability studies in 4 T1 cells

In vitro experiments to test the synergistic effect of CHO-P(MPEGA-*co*-1,2DA)-Acetal or CHO-P(MPEGA-*co*-1,3DA)-Acetal with the DOX-NP were conducted in mouse breast cancer cells (4 T1 cells). 4 T1 cells were seeded into a 96-well plate with either DOX, free formaldehyde, CHO-P (MPEGA-*co*-1,2DA) or CHO-P(MPEGA-*co*-1,3DA) polyacrylate-based prodrugs, DOX with formaldehyde (formalin solution), or DOX with the polyacrylate-based prodrug at 0.01, 0.1, 1 and 10 μg/mL were incubated for 24 h (detailed explanation given in SI). A colorimetry cell viability assay, CellTiter 96® Aqueous Non-Radioactive Cell

Proliferation Assay (MTS), was used to test cytotoxicity against a control (cells without treatment). Cell viability was measured at 495 nm with clear phosphate buffered saline (PBS) as blank samples in Perkin-Elmer HTSoft 3000 plate reader instrument.

2.2.9. Cytotoxicity evaluation and Lactate dehydrogenase assay with cardiomyocytes

In vitro experiments were conducted in neonatal rat ventricular myocytes (NRVM, P1-3) seeded in 96-well plates, where the coating with nitrocellulose is optional. The cells were treated with CHO-P (MPEGA-*co*-1,2DA) formaldehyde prodrug, free DOX and free formaldehyde drug combination and our dual delivery system at a concentration of 10 μg/mL in basal medium. Treatment solutions in complete medium were added to the seeded cells and incubated for 24 h. The supernatant was removed and used for lactate dehydrogenase (LDH) activity using a CytoTox 96 non-radioactive cytotoxicity assay (Promega). Absorbance was measured at 495 nm using Perkin-Elmer HTSoft 3000 plate reader instrument.

3. Results and discussion

To successfully deliver formaldehyde we explored methods to immobilize the gaseous compound and chemically bind it to a polymeric backbone so that premature hydrolysis and release is prevented. Therefore, we thought to form acetal units by reacting diols with the carbonyl functionality of formaldehyde. Acetal formation and cleavage is reversible, and the ring size of the acetal unit can play a role in the deprotection of the diols at lower pH. In light of this, we decided to synthesize two acetonide acrylate derivatives which can then be copolymerized successfully with a hydrophilic acrylate by RAFT polymerization [29]. Upon forming the protected polymers, the diols are deprotected and are available for post-functionalization with formaldehyde. The first protected monomer, solketal acrylate (1,2-DA), was synthesized by esterification reaction of acryloyl acrylate and solketal [30,31] (Fig. 2A). The second protected monomer, 2-(acryloyloxy) ethyl2,2,5-trimethyl-1,3-dioxane-5-carboxylate (1,3-DA), was synthesized by esterification of 2,2,5-trimethyl-1,3-dioxane-5-carboxylic anhydride [32,33] with hydroxyethyl acrylate [30] (Fig. 2B). Both monomers were obtained with considerable yield (30% and 60% respectively) and characterized using ^{1}H nuclear magnetic resonance (NMR) (Figs. S2-S3).

Each monomer, 1,2-DA or 1,3-DA, was copolymerized with poly (ethylene glycol) acrylate (MPEGA), to add hydrophilicity to the final polymer, via RAFT polymerization using 2-(n-butyltrithiocarbonate)-propionic acid (BTPA) as chain transfer reagent (Fig. 2C). The resulting polymers were copolymers in varied ratios of 60:40 and 80:20 MPEGA: (1,2- or 1,3- DA) with a molecular weight of 10,000 g/mol and reasonable dispersity of 1.10 (Table S3). For this work, we selected four polymers for our studies, two copolymers of MPEGA and 1,2-DA (P (MPEGA-*co*-1,2DA)) and two copolymers of MPEGA and 1,3-DA (P (MPEGA-*co*-1,3DA)) with ratios of 60:40 and 80:20 (Table 1).

One might question, why we not sought to prepare formaldehyde protected monomers directly which would form the desired polymers in one step. Forming the acetal from glycerol with acetone instead of using formaldehyde, avoids obtaining a glycerol formal, which contains both a 5-membered and a 6-membered acetal. However, if acetone reacts with glycerol only the 5-membered ring acetal will be favored (Fig. 2A). Therefore, the synthesis procedure has two additional synthetic steps, a deprotection step and post-modification with formaldehyde, to study both polymers with either 5-membered or 6-membered acetals incorporated (Fig. 3). The deprotection was carried out by trifluoroacetic acid at room temperature. The resulting polymers were characterized by ^{1}H nuclear magnetic resonance (NMR) and gel permeation chromatography (GPC) having molecular weights ~12 K and polydispersities (M_w/M_n) of around 1.10 for all four polymers studied (Table 1).

Post-modification of the diols was achieved by mixing the deprotected copolymers with excess formaldehyde in methanol solution to form the prodrugs (Fig. 3). An excess of 50 equivalents of formaldehyde was chosen since there is propensity to form solvent adducts and oligomers which would impede the formation of the acetal. Purification steps were conducted very carefully to remove any unattached formaldehyde using a combination of rotary evaporation, high vacuum, centrifugal filtration and lyophilization. The final conjugated material was characterized via heteronuclear single quantum correlation (HSQC) spectroscopy. HSQC provides a correlation between chemical shifts in the ^{1}H and ^{13}C NMR identifying the protons to the corresponding carbons to which they are attached. The collected spectra show two proton signals at 4.9 and 4.8 ppm for CHO-P(MPEGA-*co*-1,2DA) and 4.8 and 4.7 ppm for CHO-P(MPEGA-*co*-1,3DA) corresponding to the formaldehyde protons forming the acetals correlating to the carbon resonance at around 90 ppm. The separation of the proton signal corresponds to the difference in the chemical environment exo- and endo- to the oxygens in the ring (Figs. 4, S6). The ^{1}H NMR analysis for CHO-P(MPEGA-*co*-1,2DA) starting from 40% 1,2-DA and 20% 1,2-DA before functionalization resulted in a 25% and 20% post-functionalization efficiency. With this, we obtain two polymers yielding 9.81 wt% and 3.92 wt% formaldehyde for the 5-memberd ring acetal formaldehyde prodrug polymers. We observed a lower post-functionalization efficiency forming the 6-membered ring acetal formaldehyde prodrug of 16% and 7% for 40% 1,3-DA and 20% 1,3-DA respectively. CHO-P(MPEGA-*co*-1,3DA) with 6.45 and 1.50 wt% for 40% 1,3DA and 20% 1,3DA respectively as was obtained (Table 1).

In order to evaluate the formaldehyde release and pH responsiveness in aqueous environments, the prodrugs were suspended in either sodium acetate-acetic acid buffer (pH 5.0) or phosphate-buffered saline (PBS) (pH 7.4) inside 0.1–0.5 K MWCO dialysis Float-a-Lyzers®. The Float-a-Lyzers® were placed inside centrifugal tubes containing the corresponding release media at 37 °C from which aliquots were collected at specific times. The collected samples were analyzed via Purpald® colorimetric analysis. The Purpald® assay was chosen in this case over other techniques such as chromotropic acid or acetylacetone methods because of the superior sensitivity and being able to conduct the assay at room temperature which allowed the use of 96-well plates. According to our results, the cumulative release of formaldehyde in acidic pH is considerably faster than from physiological pH, where in the first 24 h almost 80% formaldehyde is released compared to about 10% in neutral pH (Fig. 5). After the first 24 h the released is kept constant for the duration of the experiment to around 80% in pH 5 and 10% in pH 7.4.

Table 1
Molecular weight and formaldehyde attachment data for both CHO-P(MPEGA-*co*-1,2DA) and CHO-P(MPEGA-*co*-1,3DA) at two ratios of MPEGA:DA 60:40 and 80:20.

Polymer	Monomer Feed Ratio (MPEGA:DA)	Polymer Composition[a](MPEGA: DA)	M_n[a] (g/mol)	M_n[b] (g/mol)	M_w[b] (g/mol)	M_w/M_n[b] (g/mol)	Formaldehyde (wt %)
CHO-P(MPEGA-*co*-1,2DA)	60:40	56:44	13,400	10,900	12,000	1.11	9.81
	80:20	80:20	12,400	10,600	11,400	1.08	3.92
CHO-P(MPEGA-*co*-1,3DA)	60:40	65:35	11,400	11,000	12,800	1.17	6.45
	80:20	81:19	12,300	11,100	12,400	1.11	1.50

[a] Polymer composition and M_n determined by 600 MHz ^{1}H NMR in $CDCl_3$. A detailed calculation is provided in SI.
[b] Molecular weight and polydispersity measured by GPC at 60 °C in DMF with LiBr (1 g/L) using polystyrene calibration and a flow rate of 1 mL/min. Mn_{theo} is 10,000 g/mol.

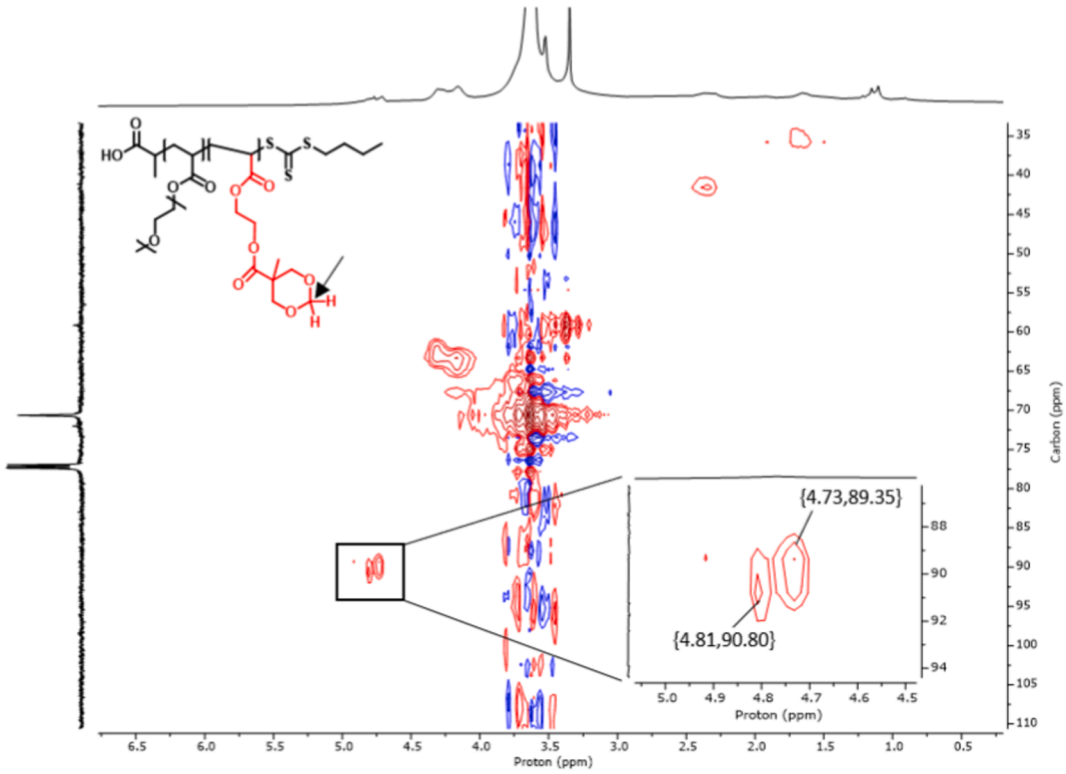

Fig. 4. Representative HSQC spectra of CHO-P(MPEGA-*co*-1,3DA) prodrug containing chemically bound formaldehyde.

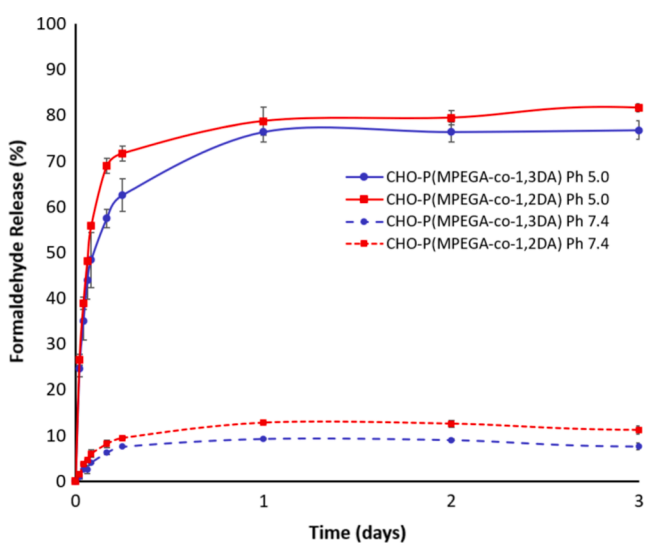

Fig. 5. Release of formaldehyde from 40% 1,2DA CHO-P(MPEGA-*co*-1,2DA) (red lines) and 40% 1,3DA CHO-P(MPEGA-*co*-1,3DA) (blue lines) prodrugs in sodium acetate-acetic acid buffer (pH 5.0) and PBS (pH 7.4) at 37 °C over 3 days. Reported values are averages of measurements in triplicate.

This result indicates that drug release is not favorable under physiological pH but instead faster in acidic conditions which is promising for applications in cancer therapies [19–21]. In addition, it is worth mentioning that there is no significant difference in the formaldehyde release between the 5-membered and the 6-membered acetal. Although the release from the CHO-P(MPEGA-*co*-1,2DA) is slightly faster, achieving 82% in 72 h compared to 77% in 72 h for CHO-P(MPEGA-*co*-1,3DA). This small difference could be attributed to the ring thermodynamic stability of the 6-membered ring in CHO-P(MPEGA-*co*-1,3DA) in comparison to the 5-membered ring in CHO-P(MPEGA-*co*-1,2DA). As an additional control, the same experiment was conducted in the presence of DOX-loaded nanoparticles, which resulted in a similar release profile (Fig. S12).

The nanoparticles were made by intermolecular crosslinking reaction of poly(δ-valerolactone-*co*-2-oxepane-1,5-dione) (P(VL-*co*-OPD)) with bis(aminooxy)PEG-3 via oxime click chemistry [27] (Fig. 6). For this project, the low concentration (2.7 mM) and an OPD percentage (8%) in the polymer backbone were chosen with the goal to form nanoparticles below 200 nm. Having nanoparticles of <200 nm has shown to be beneficial for biomedical applications due to the vascular enhance permeability and retention (EPR) effect that is associated with tumors retaining particles [34]. However, if smaller or larger sized particles are desired, the intermolecular crosslinking technique allows for an easy adjustment of the dimensions [27]. The particles formed through this crosslink reaction contain oxime bonds which are cleavable at pH 5.0 but can also be reduced to form stable alkoxyamine bonds. For this work, we chose to form particles with 50% ketoxime and 50% alkoxyamine crosslinks, because we anticipate the partial reduction of the crosslink chemistry will provide a tailored drug release and degradation profile ideal for the delivery of the DOX. We were able to obtain particles with sizes of 195 ± 65 nm according to dynamic light scattering (DLS) (Fig. S9) and 141 ± 28 nm as measured from transmission electron microscopy (TEM) (Fig. 6B).

Doxorubicin was encapsulated in the nanoparticles through a developed nanosolubilization technique in which, DOX and the nanoparticles were solubilized in minimal amount of DMSO and water containing 1 wt% D-α-tocopherol polyethylene glycol 1000 succinate. The mixture was centrifuged in two cycles to collect the DOX-loaded particle pellet and finally washed with excess water and lyophilized to remove any water remaining from the resulting DOX-loaded particles. The drug loading was determined via high performance liquid chromatography (HPLC) to be 14 wt% DOX with an average encapsulation efficiency of 68%.

The DOX-loaded particles were then used to evaluate the drug release profile and pH responsiveness at pH 5.0 and pH 7.4. The particles

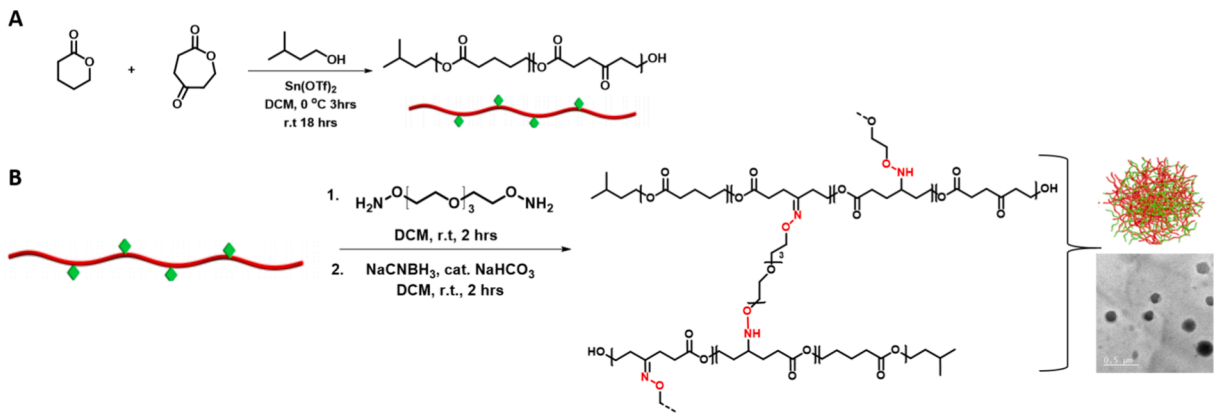

Fig. 6. (A) Synthesis of polymer precursor P(VL-*co*-OPD) via ring opening polymerization. (B) Synthesis of the partially reduced (50%) ketoxime/alkoxyamine polyester nanoparticles via oxime click chemistry. TEM image of nanoparticles measuring 141 ± 28 nm.

were suspended in either sodium acetate-acetic acid buffer (pH 5.0) or phosphate-buffered saline (PBS) (pH 7.4) both containing 0.1% v/v Tween-80 as a surfactant. Tween-80 is commonly used for drugs with poor solubility when *in vitro* release assays are being conducted, since it promotes suspension of the drug in the release media hence a more accurate release profile can be obtained when aligned with true physiological conditions [35–37]. The release profile (Fig. 7) was obtained by diluting the DOX-loaded particles in the same aqueous media as mentioned before (pH 5.0 and 7.4). A faster release is exhibited at acidic pH 5.0 in which almost 80% cumulative DOX release is obtained in the first 72 h and maintained for the total duration of the experiment. Whereas a slower release is achieved under physiological pH with a maximum cumulative release of around 8% DOX in the first 24 h and is constant throughout the remaining duration of the experiment. The pH responsiveness of the drug release experiment complements the result of the formaldehyde release from prodrugs and is considered a promising result in the pursuit to establish a synergistic release system of DOX and formaldehyde. The presence of the formaldehyde prodrug in the DOX release studies did not affect the release profile (Fig. S13). Although we designed the dual delivery system, carrying each drug in separate and for each drug the most optimized system, the action of the two drugs is unified by the pH guided release mechanism by which each drug is released in the same environment at a comparable rate with the intent to work in synergy.

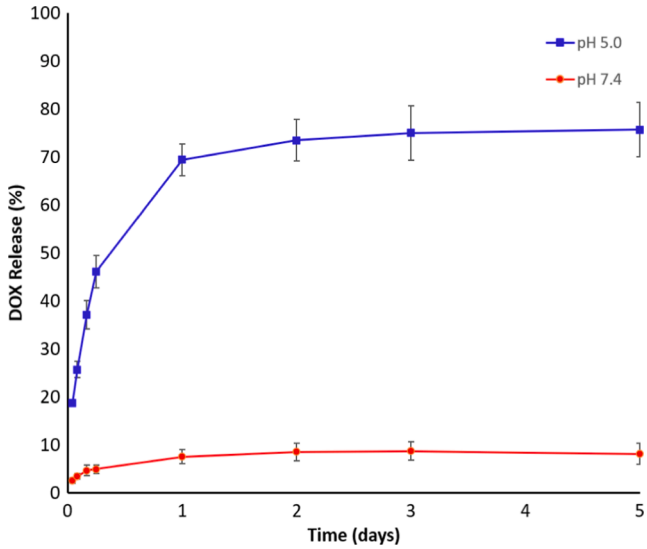

Fig. 7. Release of DOX from partially reduced 8% OPD, 2.7 mM ketoxime/alkoxyamine nanoparticles in sodium acetate-acetic acid buffer (pH 5.0) (blue line) and PBS (pH 7.4) (red line) containing 0.1% v/v Tween-80 at 37 °C over 5 days reported as an average of measurements in triplicate.

Finally, to analyze the dual effect of DOX-loaded particles and formaldehyde prodrugs, cell cytotoxicity experiments were conducted in mammalian breast cancer cells (4 T1). Previous work with DoxF and DoxSF has shown that only one equivalent of formaldehyde is necessary to form the DOX precursor that results in the DOX-DNA adduct [15]. Therefore, we chose a 1:1 ratio of DOX-NP to formaldehyde prodrugs to study the cytotoxicity of our drug combination. In order to confirm that the active DOX-formaldehyde prodrug is formed with only one equivalent and additional formaldehyde does not significant affect the overall treatment response, a cytotoxicity study of our dual delivery system was conducted at varying DOX:F ratios of 1:1, 1:2 and 1:50. Results indicated a minimal decrease in percent viability as more formaldehyde(1:2) is used, and an increase up to 50 equivalents of formaldehyde did not show any significant effect (Fig. 8A). We concluded that additional formaldehyde does not increase the efficacy of the drug combination.

The cell viability assay was conducted with 4 T1 cells which were incubated in 96-well plates for 3 h for cell attachment and then treated with different media containing free DOX, DOX + formaldehyde, DOX-NP + formaldehyde, DOX + CHO-P(MPEGA-*co*-1,2DA) or CHO-P (MPEGA-*co*-1,3DA), DOX-NP + CHO-P(MPEGA-*co*-1,2DA) or CHO-P (MPEGA-*co*-1,3DA) in concentrations of 0.01, 0.1 1, and 10 μg/mL and incubated for 24 h (Figs. 8B, S11). After 24 h the media containing drug formulations was aspirated and replaced with 20 μL of MTS reagent containing phenazine methosulfate (PMS) in 100 μL complete media and incubated for about 1 h then absorbance was measured at 490 nm. Analysing the results, co-administration of free DOX and free formaldehyde showed a significant decrease in the cancer cell growth, with free DOX achieving about 60.6 ± 1.7% cell cytotoxicity against 30.7 ± 1.8% of the co-administration (Fig. 8C). Next, we studied a combination of the DOX-NP with free formaldehyde. The free formaldehyde administered to the cells was molecular biology grade 36.5–38% formaldehyde solution in water. Here, we could observe that the sustained release of the DOX had an advantageous effect in further inhibiting cancer cell growth. The dual drug combination of DOX-NP and formaldehyde prodrug was administered concerted to allow the immediate formation of the DOX-Schiff's base which is anticipated to rapidly enter the cancer cell to form the desired DOX-DNA adducts. The cell viability assay confirmed the synergistic effect of both DOX and formaldehyde. Our drug combination showed a 4-fold increase in cancer cell cytotoxicity compared to free DOX and with free formaldehyde together (2-fold) (Fig. 8C). IC_{50} values obtained via regression analysis also corroborate our results of an around 4-fold increase in cell death for our dual delivery system (Fig. 8F). When comparing both polymers evaluated in this study, CHO-P(MPEGA-*co*-1,2DA) shows a slightly higher percentile of cancer cell death of 15.9 ± 1.40% against 18.3 ± 3.24% of CHO-P

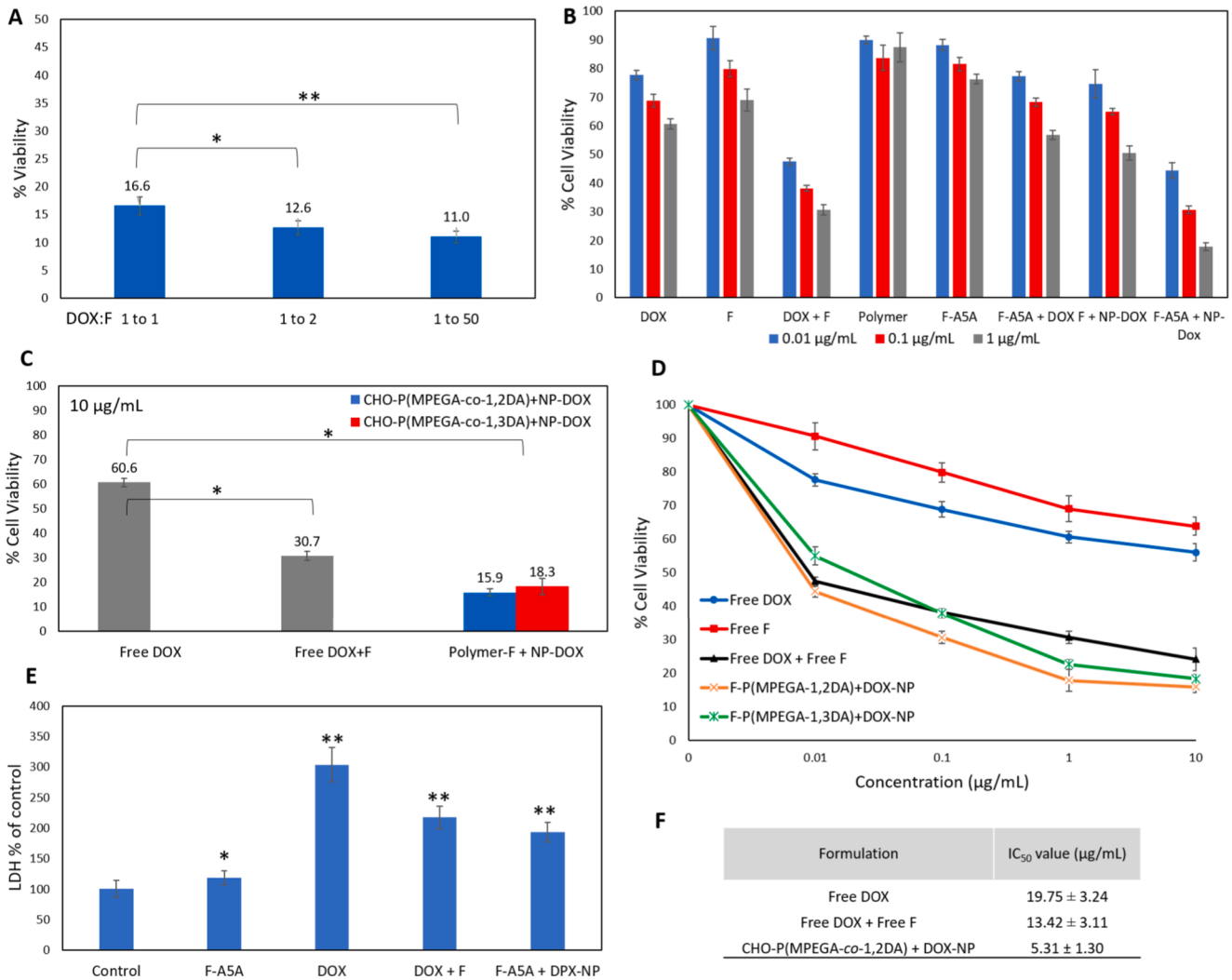

Formulation	IC_{50} value (µg/mL)
Free DOX	19.75 ± 3.24
Free DOX + Free F	13.42 ± 3.11
CHO-P(MPEGA-*co*-1,2DA) + DOX-NP	5.31 ± 1.30

Fig. 8. (A) Cytotoxicity study at different DOX:Formaldehyde ratios of the dual delivery system (CHO-P(MPEGA-*co*-1,2DA) and DOX-NP) at a concentration of 10 µg/mL in 4 T1 cells after 24 h. Asterisks indicate statistical significance; a single asterisk (*) at *p*-value < 0.05 and a double asterisk (**) at *p*-value <0.01 determined via one-tailed *t* test performed using two-sample unequal variance. (B) Complete cell viability assay for CHO-P(MPEGA-*co*-1,2DA) prodrug at concentrations of 0.01, 0.1 and 1 µg/mL after 24 h in 4 T1 cells in combination with DOX-NP. (C) Cell viability to evaluate efficacy of resulting polymer matrix CHO-P(MPEGA-*co*-1,2DA) + DOX-loaded NP and combined CHO-P(MPEGA-*co*-1,3DA) + DOX-loaded NP compared to free DOX and free combined DOX + F at a concentration of 10 µg/mL. Asterisks indicate statistical significance; a single asterisk (*) at *p*-value <0.05 and a double asterisk (**) at *p*-value < 0.01 determined via two-tailed *t* test performed using two-sample unequal variance. (D) Cell cytotoxicity of free DOX, free formaldehyde (F), combined free DOX and F (1:1), combined CHO-P(MPEGA-*co*-1,2DA) and DOX-loaded NP and combined CHO-P(MPEGA-*co*-1,3DA) and DOX-loaded NP after 24 hrs at varying concentrations. (E) Lactic Acid Dehydrogenase (LDH) levels in neonatal rat ventricular myocytes. LDH % of untreated control, CHO- P(MPEGA-*co*-1,2DA) formaldehyde prodrug, free DOX, free drug combination and dual delivery system. ** *p*-values < 0.01 vs control, * *p*-values < 0.05 vs control. (F) IC_{50} values of free DOX, combination of free DOX and free F, and our drug delivery system upon treatment with 4 T1 cells. Data expressed as a mean ± SD (n = 4). Each data point represents an average of measurements in triplicates.

(MPEGA-*co*-1,3DA), however this difference is within the error and therefore limited. We attribute this slight difference to the faster release of the 5-membered ring in contrasts to the 6-membered ring polymer and therefore CHO-P(MPEGA-*co*-1,2DA) matches to a higher degree that of DOX-NP.

At higher concentrations the increased efficacy of the dual system towards cancer cell viability becomes more prevalent and the result underlines that the two drug formulations have a higher ability to form the DNA-adduct with a higher success in inhibiting cancer cell proliferation (Fig. 8D). The dual release system allows the continuous formation of the DOX-formaldehyde reactive intermediate over a period of 6 h. This is achieved to a lesser degree with either the two free drugs or the DOX-NP and free formaldehyde (Fig. S10). The other advantage establishing this mechanism of action for the two active compounds is the associated effect of a lowered cardiotoxicity of DOX. The profound effect of formaldehyde is an enabling mechanism to bind DOX to the DNA and with this sequester DOX to the nucleus and reducing the DOX availability in the mitochondria as well as in the bloodstream, preventing redox-cycling and ROS. It leads to the working hypothesis that formation of DOX- DNA adduct limits the damage of cardiomyocytes [11–14]. To test this this effect *in vitro*, the lactase dehydrogenase (LDH) activity, as an indicator of tissue damage, is tested in a Lactate dehydrogenase assay if in this dual delivery system, formaldehyde is capable to play a central role in protecting in neonatal rat ventricular myocytes. A high level of LDH activity points to acute cell damage. A previous small molecule study by A. Rephaeli and coworkers showed that the combination of DOX with a small molecule formaldehyde prodrug reduced the cardiotoxicity associated with DOX administration [10]. We were able to conduct similar experiments with comparable results in which it is evident that the combination of formaldehyde and DOX results in a reduced cardiotoxicity. Additionally, our delivery system combination achieves a reduced cardiotoxicity in the cardiomyocytes

similar to that of the free components (free DOX and free formaldehyde) with a slightly improvement. It is also worth mentioning that similar to previous literature [10] the formaldehyde prodrug alone did not show damage to the cells and from our results it is evident that the highest toxicity is attributed to the administration of DOX and not formaldehyde, whereby the formation of the DOX-formaldehyde intermediate has a great effect in cardiomyocyte protection. (Fig. 8E). The drug combination delivery system allows for a controlled delivery and sustained release of both DOX and formaldehyde in a more efficient manner and thereby reducing the cardiotoxicity of the DOX and at the same time increasing the efficiency of DOX by 4-fold.

4. Conclusions

In conclusion, we have demonstrated the successful design of a pH-responsive dual delivery system triggering the release of DOX and formaldehyde at pH 5.0, mimicking the extracellular matrix of tumors. This was made possible by combining polyacrylate-formaldehyde prodrugs with polyester nanoparticles with partially reduced ketoxime/alkoxyamine crosslinks that can encapsulate DOX. Matching release kinetics favored the formation of the DOX-formaldehyde active intermediate (DOX-DNA adduct) to result in the maximum cell death rate (4-fold) in comparison to co-administration of free DOX and free formaldehyde (2-fold). The pH-trigger will allow a concerted release of the therapeutics at the place of action. Supporting the sustained release mechanism was the observation of the higher effect of the prodrug combination in contrast to free drug combinations at higher concentrations of 10 μg/mL. We can conclude that this is the first example of a polymeric pH triggered formaldehyde prodrug that has the potential to significantly reduce the limiting clinically impact due to severe cardiotoxicity and at the same time improving the therapeutic index of DOX using pharmacological insights of the interplay of formaldehyde and DOX.

CRediT authorship contribution statement

Estela Ordonez: Conceptualization, Software, Validation, Formal analysis, Investigation, Writing - review & editing, Visualization. **Laken L. Kendrick-Williams:** Conceptualization, Investigation. **Eva Harth:** Conceptualization, Methodology, Validation, Resources, Data Curation, Writing - original draft, Writing - review & editing, Supervision, Project administration, Funding acquisition.

Declaration of Competing Interest

The authors declare that they have no known competing financial interests or personal relationships that could have appeared to influence the work reported in this paper.

Acknowledgements

The authors thank the Robert A. Welch Foundation for the generous support of this research (#H-E-0041) through the UH Center of Excellence in Polymer Chemistry. The authors also thank the National Science Foundation (CHE-1808664) for support. The authors also thank the Dr. Randall Lee laboratory for assistance and access to the Malvern Zetasizer Nanosystem analysis (Defense University Research Instrumentation Program grant (FA9550-15-1-0374) issued by the Air Force Office of Scientific Research). We also would like to thank Dr. Chengzhi Cai laboratory for giving us access to the Perkin Elmer Bio-Assay plate reader.

Appendix A. Supplementary material

Supplementary data to this article can be found online at https://doi.org/10.1016/j.eurpolymj.2020.110210.

References

[1] J. Lehár, A.S. Krueger, W. Avery, A.M. Heilbut, L.M. Johansen, E.R. Price, R. J. Rickles, G.F. Short Iii, J.E. Staunton, X. Jin, M.S. Lee, G.R. Zimmermann, A. A. Borisy, Nat. Biotechnol. 27 (2009) 659–666.
[2] J. Foucquier, M. Guedj, Pharmacol. Res. Perspect. 3 (2015) e00149.
[3] O. Tacar, P. Sriamornsak, C.R. Dass, J. Pharm. Pharmacol. 65 (2013) 157–170.
[4] R.D. Olson, P.S. Mushlin, FASEB J. 4 (1990) 3076–3086.
[5] O.J. Arola, A. Saraste, K. Pulkki, M. Kallajoki, M. Parvinen, L.-M. Voipio-Pulkki, Cancer Res. 60 (2000) 1789–1792.
[6] L. Smith, M.B. Watson, S.L. Kane, P.J. Drew, M.J. Lind, L. Cawkwell, Mol. Cancer Ther. 5 (2006) 2115–2120.
[7] H.E. Mohamed, S.E. El-Swefy, H.H. Hagar, Pharmacol. Res. Commun. 42 (2000) 115–121.
[8] G. Minotti, R. Ronchi, E. Salvatorelli, P. Menna, G. Cairo, Cancer Res. 61 (2001) 8422–8428.
[9] L. Steinherz, P. Steinherz, Pediatrician 18 (1991) 49–52.
[10] A. Rephaeli, S. Waks-Yona, A. Nudelman, I. Tarasenko, N. Tarasenko, D. Phillips, S. Cutts, G. Kessler-Icekson, Br. J. Cancer 96 (2007) 1667–1674.
[11] S.M. Cutts, L.P. Swift, V. Pillay, R.A. Forrest, A. Nudelman, A. Rephaeli, D. R. Phillips, Mol. Cancer Ther. 6 (2007) 1450–1459.
[12] D. Engel, A. Nudelman, I. Levovich, T. Gruss-Fischer, M. Entin-Meer, D.R. Phillips, S.M. Cutts, A. Rephaeli, J. Cancer. Res. Clin. 132 (2006) 673–683.
[13] A. Rephaeli, M. Entin-Meer, D. Angel, N. Tarasenko, T. Gruss-Fischer, I. Bruachman, D.R. Phillips, S.M. Cutts, D. Haas-Kogan, A. Nudelman, Invest. New Drugs 24 (2006) 383–392.
[14] S.M. Cutts, A. Rephaeli, A. Nudelman, I. Hmelnitsky, D.R. Phillips, Cancer Res. 61 (2001) 8194–8202.
[15] G.C. Post, B.L. Barthel, D.J. Burkhart, J.R. Hagadorn, T.H. Koch, J. Med. Chem. 48 (2005) 7648–7657.
[16] D.J. Fenick, D.J. Taatjes, T.H. Koch, J. Med. Chem. 40 (1997) 2452–2461.
[17] S.M. Cutts, A. Nudelman, A. Rephaeli, D.R. Phillips, IUBMB Life 57 (2005) 73–81.
[18] B.L. Barthel, E.L. Mooz, L.E. Wiener, G.G. Koch, T.H. Koch, J. Med. Chem. 59 (2016) 2205–2221.
[19] A.S.E. Ojugo, P.M.J. McSheehy, D.J.O. McIntyre, C. McCoy, M. Stubbs, M.O. Leach, I.R. Judson, J.R. Griffiths, NMR Biomed. 12 (1999) 495–504.
[20] T. Fukamachi, Y. Chiba, X. Wang, H. Saito, M. Tagawa, H. Kobayashi, Cancer Lett. 297 (2010) 182–189.
[21] Xiaomeng Zhang, Y.L. A. R.J. G., J. Nucl. Med.51 (2010) 1167–1170.
[22] D. Nguyen, C. Boyer, ACS Biomater. Sci. Eng. 1 (2015) 895–913.
[23] W.-P. Li, C.-H. Su, L.-C. Tsao, C.-T. Chang, Y.-P. Hsu, C.-S. Yeh, ACS Nano 10 (2016) 11027–11036.
[24] H.T. Duong, Z.M. Kamarudin, R.B. Erlich, Y. Li, M.W. Jones, M. Kavallaris, C. Boyer, T.P. Davis, Chem. Comm. 49 (2013) 4190–4192.
[25] M.N. Mann, B.H. Neufeld, M.J. Hawker, A. Pegalajar-Jurado, L.N. Paricio, M. M. Reynolds, E.R. Fisher, Biointerphases 11 (2016) 031005.
[26] W. Du, K. Zhang, S. Zhang, R. Wang, Y. Nie, H. Tao, Z. Han, L. Liang, D. Wang, J. Liu, N. Liu, Z. Han, D. Kong, Q. Zhao, Z. Li, Biomaterials 133 (2017) 70–81.
[27] L.L. Kendrick-Williams, E. Harth, Macromolecules 51 (2018) 10160–10166.
[28] J. Niu, D.J. Lunn, A. Pusuluri, J.I. Yoo, M.A. O'Malley, S. Mitragotri, H.T. Soh, C. J. Hawker, Nat. Chem. 9 (2017) 537–545.
[29] D. Nguyen, T.-K. Nguyen, S.A. Rice, C. Boyer, Biomacromolecules 16 (2015) 2776–2786.
[30] Y. Xu, Y.J. Hong, D.J. Tantillo, M.K. Brown, Org. Lett. 19 (2017) 3703–3706.
[31] N.A.A. Rossi, Y. Zou, M.D. Scott, J.N. Kizhakkedathu, Macromolecules 41 (2008) 5272–5282.
[32] L.I. Ronco, A. Basterretxea, D. Mantione, R.H. Aguirresarobe, R.J. Minari, L. M. Gugliotta, D. Mecerreyes, H. Sardon, Polymer 122 (2017) 117–124.
[33] H. Ihre, A. Hult, J.M.J. Fréchet, I. Gitsov, Macromolecules 31 (1998) 4061–4068.
[34] J. Fang, H. Nakamura, H. Maeda, Adv. Drug Delivery Rev. 63 (2011) 136–151.
[35] S.A. Abouelmagd, B. Sun, A.C. Chang, Y.J. Ku, Y. Yeo, Mol. Pharmaceutics 12 (2015) 997–1003.
[36] Ketan T. Savjani, A.K. G., Jignasa K. Savjani, ISRN Pharm. (2012) 1–10.
[37] Sivaram Nallamolu, V.R. J., Mallikarjun Chitneni, Prashant Kesharwani, ASPS 2 (2018) 2–13.